The Ringed Spiral Galaxy NGC4622. II. An Independent Determination That the Two Outer Arms Lead

Gene G. Byrd – University of Alabama

Tarsh Freeman – Bevill State Community College

Sethanne Howard – U. S. Naval Observatory, Washington

Ronald J. Buta – University of Alabama

Citation of published version:

Byrd, G., Freeman, T., Howard, S., Buta, R. (2007): The Ringed Spiral Galaxy NGC4622. II. An Independent Determination That the Two Outer Arms Lead. *The Astronomical Journal*, 135(1). DOI: 10.1088/0004-6256/135/1/408

The Astronomical Journal, 135:408–413, 2008 January doi:10.1088/0004-6256/135/1/408

THE RINGED SPIRAL GALAXY NGC4622. II. AN INDEPENDENT DETERMINATION THAT THE TWO OUTER ARMS LEAD

Gene G. Byrd[1], Tarsh Freeman[2], Sethanne Howard[3,4], and Ronald J. Buta[1]
[1] Department of Physics and Astronomy, University of Alabama, Tuscaloosa, AL 35487, USA; byrd@bama.ua.edu
[2] Bevill State Community College, Jasper, AL 35555, USA
[3] 5526 Green Dory Lane, Columbia, MD 21044, USA
Received 2006 September 3; accepted 2007 October 30; published 2007 December 12

ABSTRACT

The spiral galaxy NGC4622 was recognized by Byrd et al. (1989, Celest. Mech., 45, 31) to have a single inner arm winding outward counterclockwise (CCW) and an outer pair of arms winding outward clockwise (CW). Using *HST* and ground-based observations, Buta et al. (2003, AJ, 125, 634) used a dust silhouette method to determine that the disk of NGC4622 rotates CW on the sky. The outer pair of arms winding outward CW on the sky should thus lead (wind outward in the direction of disk orbital motion), contrary to most expectations. We have discovered in Fourier component images an additional pair of weak CCW arms: this pair is inside the already-known strong outer CW pair. We also find an additional weak single CW arm component: this arm is outside the strong, already-known, CCW single inner arm. Thus, regardless of disk rotation sense, NGC4622 has a pair of leading arms as well as a single leading arm. NGC4622's moderate (19°) tilt is a plus for the methods in the present paper. We use a well-demonstrated *IVB* color/age method to locate co-rotation (CR) radii. At CR, the Fourier position angle peaks switch position angle sequence (e.g., *IVB* to *BVI* or the reverse). We find two possible CR radii (21.4″ and 36″). The boundary between the outer CW arms and the inner CCW arms is between these two radii. From the *IVB* switching senses crossing the CR radii and the observed orbital angular rate decline with increasing radius across the first CR, the orbit sense is CW and the outer pair thus is the leading pair. We thus place on a firm footing for future research our earlier conclusions about the unusual nature of the NGC4622 spiral pattern.

Key words: galaxies individual (NGC4622) – galaxies: spiral – galaxies: structure

1. INTRODUCTION

The winding of spiral arms is an important dynamical and kinematic feature of any spiral galaxy. Whether arms trail or lead the direction of rotation of the disk has been of interest since spirals were first noticed. Trailing is defined as winding outward opposite the sense of disk orbital motion; leading is winding outward in the same sense.

Historically, astronomers took both viewpoints. Based on theoretical studies, Lindblad (1941) concluded that spiral arms are usually leading. Hubble (1943) came to the opposite conclusion: that arms are generally trailing. Based on kinematic studies where one can unambiguously distinguish the near side of the disk of nearly edge-on galaxies, de Vaucouleurs (1958) also determined that arms are trailing. He used the observed asymmetry in the dust distribution to determine which side of the disk minor axis is the near side. It is presumed that the actual dust distribution is bi-symmetric in the disk plane. The apparent dust asymmetry is caused by the fact that, in an inclined galaxy, dust in the near side is silhouetted against the background starlight of the bulge and disk. This determination, combined with the apparent arm winding sense being outward clockwise (CW) or counterclockwise (CCW) on the sky plus Doppler shift observations, permitted de Vaucouleurs to verify that all the arms in his sample trailed. In galaxies with significant nearly spherical bulge components, this silhouette effect can be seen even if the galaxy is more nearly face-on.

In their discussion of density wave theory, Binney & Tremaine (1987) argue that leading arms are not likely to be seen because they would quickly unwind and become trailing arms. However, theoretical studies indicate (e.g., Athanassoula 1978 and references therein) that strong (i.e., massive perturber) retrograde tidal encounters (opposite the disk rotation sense) can generate a leading arm near the $m = 1$ inner Lindblad resonance. Self-gravitating n-body simulations (Byrd et al. 1989; Thomasson et al. 1989) support the theory by showing that strong retrograde encounters in the presence of a large halo-to-disk mass ratio can produce a leading arm, particularly in the region of the +1:1 co-rotational (CR) resonance of the disk material's orbital and epicyclic motion with the angular velocity of the perturber passing by a flat rotation curve disk. If disk self-gravity is significant, trailing arms result even for strong retrograde encounters. Although leading arms do have a theoretical basis, the general consensus still has been that spiral arms trail, most particularly, pairs of arms. An $m = 2$ trailing spiral density wave is most effective at transporting angular momentum outwards.

Byrd et al. (1993) argue that retrograde companions ought to be as frequent as prograde companions with random encounter directions. Keel (1991) determined that retrograde and prograde companions are equally common in a sample of Karachentsev pairs. Thomasson et al. (1989) suggest that approximately 25% of spirals with major companions should have a leading arm, not the observed fraction of de Vaucouleurs. There is thus a discordance between (1) the fraction of retrograde companions, (2) Thomasson et al.'s result that these companions should trigger leading arms, and (3) the failure of de Vaucouleurs to find leading arms.

A galaxy that definitely has a leading arm or arms will help to clarify this issue. NGC4622 is a southern, ringed spiral galaxy (type SA(r)a) in the Centaurus cluster about 40 Mpc distant. It has two strong CW-winding arms wrapping around a large bulge. As is typical of such Sa galaxies, the bulge contributes about half of the light. The galaxy is almost face-on with an

[4] Retired from U.S. Naval Observatory, Washington, DC, USA.

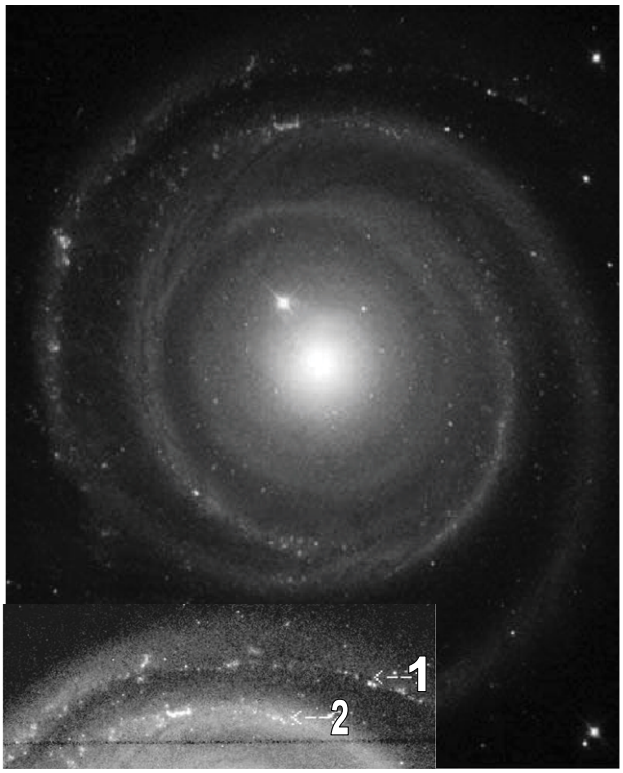

Figure 1. Black and white version of the Hubble Heritage image based on the F336W, F439W, F555W, and F814W WFPC images of NGC4622. North is oriented 30° clockwise from the top vertical with east 90° CCW from north. The numbers in the lower inset mark where blue associations are on the interior (1) and exterior (2) of the smooth yellow outer pair of arms. The horizontal stripe is an artifact.

inclination about 19° (Buta et al. 2003). Figure 1 shows the *HST* Hubble Heritage image of this galaxy.

As noted by Buta et al. (1992), NGC4622 provides one of the most convincing cases of a leading spiral arm or arms in *any* galaxy. In a blue-sensitive, ground-based image of NGC4622, Byrd et al. (1989) pointed out that, in addition to the pair of strong, outer arms winding outward CW, NGC4622 has a weaker, single inner arm winding outward CCW inside a ring. Using multi-band ground-based surface photometry, Buta et al. (1992) showed observationally that the single inner arm is a feature in the stellar disk, not the result of a chance distribution of young stars or gas. Clearly for NGC4622, either the outer arms lead and the inner arm trails, or the outer arms trail and the inner arm leads.

Accepting the consensus that pairs of arms trail, Byrd et al. (1993, BFH) provided an *n*-body simulation which produced a single leading inner arm and two outer trailing arms. They used a fully self-gravitating *n*-body code with a 2D Mestel disk of "stars" and "gas" cloud components and a point-mass companion that moves in three dimensions. They found that a retrograde encounter with a massive perturber cannot form *both* trailing and leading arms in one galaxy. To reproduce the NGC4622 two-way structure, BFH needed a massive halo (with the disk having only 1/8 that needed to produce a flat rotation curve and the halo making up the difference) with a plunging retrograde encounter of a small (1/100 the mass of the disk) perturber along the plane of the disk. This retrograde perturber produced a single inner leading and outer trailing pair of arms for a flat rotation curve. They found that a direct plunging disk plane passage of a low-mass perturber will produce a single *trailing* arm in the inner disk, and again, a trailing pair in the outer disk. Plunging encounters by small perturbers can create leading or trailing single central arms.

2. PREVIOUS OBSERVATIONAL VERIFICATION OF LEADING ARMS

As a result of the ground-based multi-band photometry of the stellar disk, and the BFH simulations, the situation with NGC4622 was thought to be settled. To double check the conclusions, Buta et al. (2003, hereafter paper I) obtained four new sets of observations: *HST* WFPC2 images in *UBVI*, a CTIO Fabry–Perot Hα velocity field, CTIO *BIH* images, and Parkes 64 m 21 cm data. Using these observations, paper I gave the surprising result that the two clockwise-opening outer arms are *leading* instead of trailing. This means, therefore, that the inner arm trails. To show this, paper I uses the dust silhouette and Doppler shift method outlined by de Vaucouleurs (1958). The method involves (1) determining the receding and approaching halves of the disk through Doppler shifts along the line of nodes, and (2) identification of the near side of the disk using disk plane dust reddening and cloud silhouettes against the large bulge of NGC4622. Even though it does have an unusual arm pattern, NGC4622 is not totally unique. There are at least three other galaxies that show features in common with NGC4622's spiral pattern: e.g., the Blackeye Galaxy (NGC4826), ESO 297-27, and NGC3124 (see paper I for a description of these galaxies).

Except for the odd winding of the spiral arms, there is little evidence of disruption in the NGC4622 disk. NGC4622 has remarkably smooth arms. However, the galaxy's outer parts are slightly lop-sided. Also NGC4622's short central dust lane (see paper I) may indicate a past merger or tidal stripping. There is a small companion of unknown redshift near NGC4622 on the sky. We plan to study this further via simulations in a later paper. Because the conclusions of paper I are so unusual, in this paper, paper II, we simply concentrate on substantiating them by independent methods.

3. ROTATION CURVE

We begin with the NGC4622 rotation curve. Figure 2 shows the de-projected rotation curve on (from paper I, Table 1). It is fairly flat in the inner portions, then rising in the outer part of the disk. This outer portion is a controversial result. Poor fits to the observed de-projected rotation curve were obtained in paper I with conventional flat or declining rotation curves in the outer portions. Because NGC4622 is not a highly inclined galaxy, warping of the outer disk by amounts comparable to the 19° inclination of the galaxy might lead to erroneous conclusions about the outer rotation curve. Figure 3 shows a plot of the orbital angular velocity versus radius corresponding to the Figure 2 rotation curve. Even considering the standard deviation limits, note that the angular rate certainly declines perhaps as far out as a 30″ radius. This decline is reasonable and common. As can be seen in the figure, the angular rate may then rise at larger radii than 30″.

Is the NGC4622 disk flat? As can be seen in Figure 4 (paper I's Figure 13), the radial velocity contours over the NGC4622 disk are much what one would expect from a tilted flat disk of material in circular orbits. The contours of constant radial velocity are fairly symmetric about the disk line of nodes and minor axis. However, as we shall show, we can determine the existence of a pair of leading arms in NGC4622 without using the rotation curve.

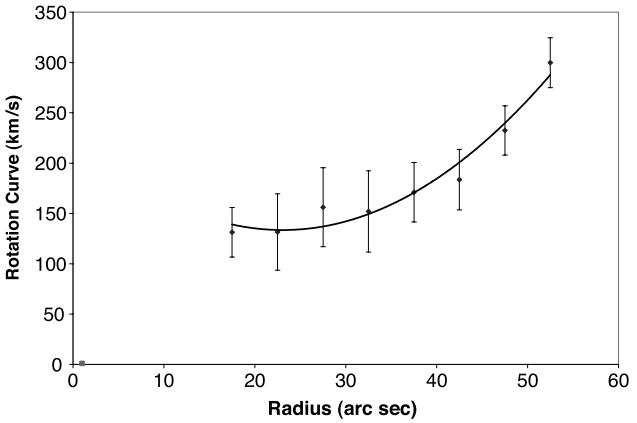

Figure 2. NGC4622's deprojected rotation curve in km s^{-1} from Table 1 of paper I fitted with a polynomial. The horizontal scale is the arcsec distance from the center along the line of nodes in the disk plane. The "error bars" indicate the standard deviation of the data points.

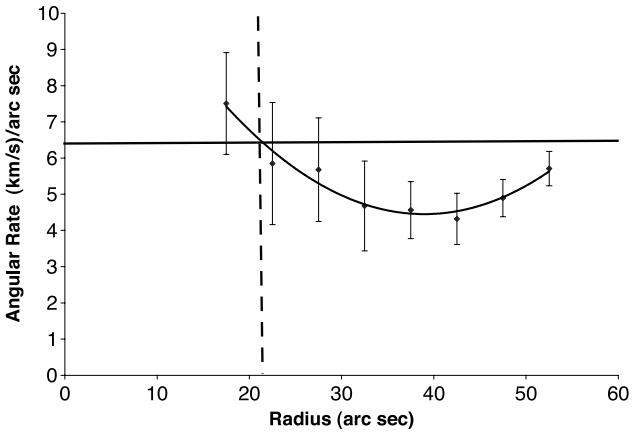

Figure 3. NGC4622's orbital angular rate in (km s^{-1})/″ versus radius in arcsec from Figure 1 fitted with a polynomial. The horizontal line indicates the presumed pattern speed of the $m = 1$ and 2 disturbance. The vertical line indicates the 21.4″ CR radius. The "error bars" are the standard deviation of the orbital angular rates computed from the Figure 2 data points.

4. CR RADII AND ARM SENSE FROM FOURIER COMPONENT *IVB* PLOTS

To identify co-rotation radii in NGC4622, we will use a color/angular sequence method proposed by Puerari & Dottori (1997; see also Vera-Villamizar et al. 2001). The method examines the position angle around the nucleus in the deprojected face-on disk of blue newly-formed ("lit-up") main-sequence stars relative to an *I*-band density wave or bar pattern. The angle between these two peaks results from a time lag between a proto-star's formation during a collision of two gas clouds in the stellar density peak and that object's contraction to the main sequence to "light-up" in blue wavelengths as a luminous main-sequence star, as first noted by Byrd et al. (1993) in NGC4622. The difference between the two will be in opposite senses inside and outside a co-rotation (CR) radius of orbital motion and pattern angular rates. This will be faster inside CR and slower outside CR for a rotation curve whose angular rate declines with increasing radius in this part of the disk. The opposite will occur if the rotation curve angular rate rises with increasing radius. In the Fourier component images we use in the present paper, starting from zero position angle and proceeding in the orbit direction relative to the pattern motion, first

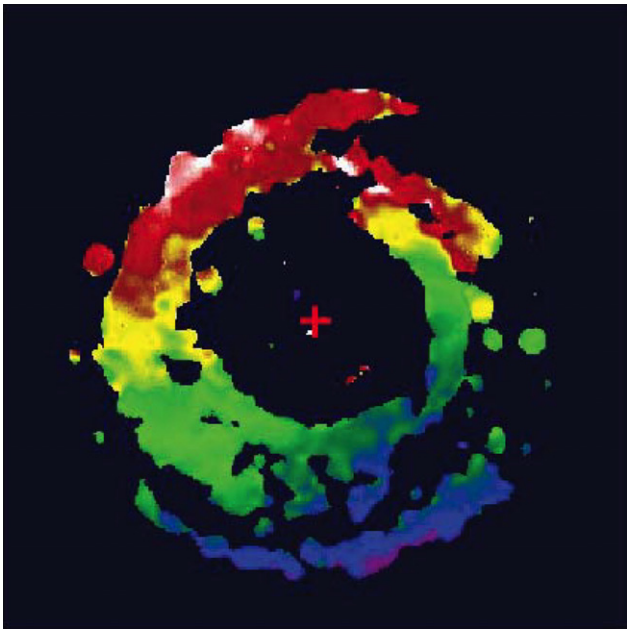

Figure 4. Hα velocity field over the disk of NGC4622. The red extreme corresponds to 4550 km s^{-1} and blue extreme corresponds to 4450 km s^{-1} relative to the nucleus with white and violet, respectively, representing the extremes. The line of nodes is 22° left (eastward) from the top (north) extending to the lower right, bottom (∼SW).

to come is the intensity peak of the stellar component (*I*), then further downstream the peak of the *V* component, and finally, the *B* component peak representing bright main-sequence stars. So the color/age sequence is *IVB*.

In especially clear cases, there may be blue associations clearly displaced to one side of the stellar spiral arm. This behavior is seen in NGC4622. The inset in Figure 1 gives a deeper image of the top two arms in the larger frame Figure 1. To the left of the arm labeled "1," the blue associations are systematically displaced on the concave side of the smoother stellar arms. We will discuss this more in Section 5.

To use the *IVB* method, we must assume that NGC4622 disk and the arm pattern speed does not change greatly over times comparable to the circular orbital period (∼190 million years) at CR. Byrd et al. (2006) have verified the color sequence method with *HST* observations of *IVB* color bands in the rotating barred potential of the galaxy NGC3081. For this galaxy, whose rotation curve is clear and whose dynamics are well understood, the nearer edge of the disk relative to the sky plane is known. This, along with the velocity field, determines the disk orbit sense on the sky (CCW for NGC3081). The flat rotation curve's angular rate declines with increasing radius. The expected CCW *IVB* color/age sequence is seen for the inner ring material inside CR.

5. FOURIER IMAGES OF NGC4622 AND LEADING/TRAILING $m = 2$ ARMS

Fourier decomposition can provide a method independent of that of paper I to ascertain that one pair of arms in NGC4622 definitely leads. Figure 5 shows an *I*-band image of the Fourier $m = 2$ component of NGC4622. This filtering process reveals the underlying stellar disk, showing the already-known outer pair of CW arms. One of these is marked with white dots. In addition to the two bright outer arms, note that the $m = 2$ image

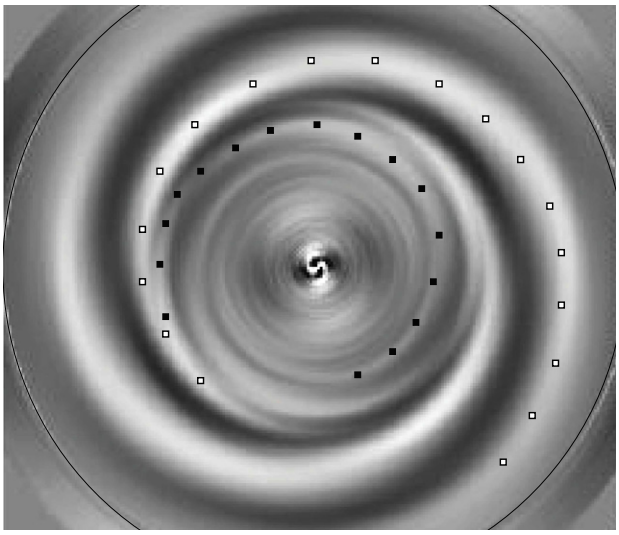

Figure 5. $m = 2$ Fourier component of a WFPC2 *I*-band image of NGC4622. North is upper right, and east is upper left. The frame covers a field of $1'.50 \times 1'.43$, stretched to a square. One of the pair of CW arms is marked with white dots. Inside about $25''$ (where the orbital angular rate declines with increasing radius), one of a possible pair of CCW (presumably trailing) arms is marked with black dots.

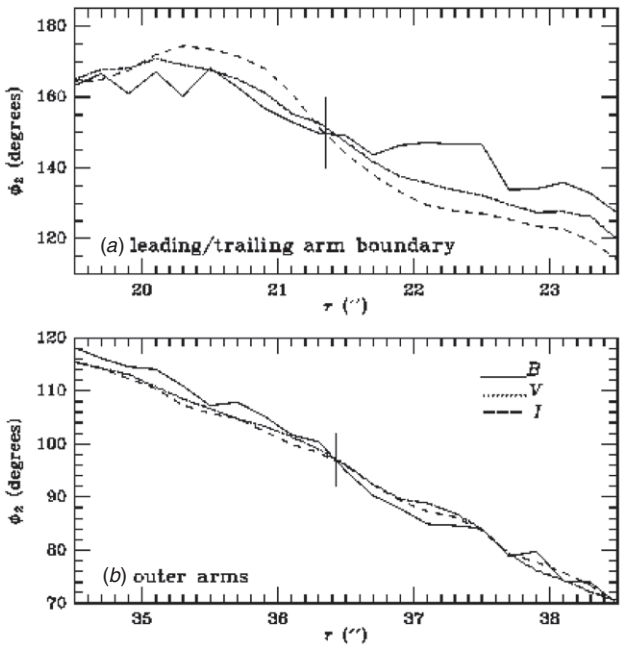

Figure 6. Position angle versus radius, for the $m = 2$ *VBI* intensities for two sections of the disk. The top shows the region $r = 20''$ to $23''$, and the bottom shows $r = 35''$ to $38''$. Note relative position angles for different *B* (——), *V* (· · · · · ·), and *I* (- - - -) color bands on each side of $21.4''$ and $36.5''$

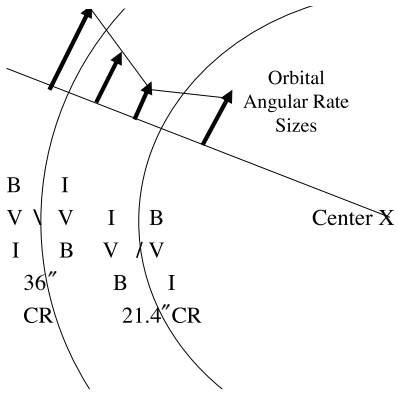

Figure 7. *IVB* "light up" sequence diagram inside and outside the $21.4''$ CR of the CW turning disturbance. *I*, *V*, and *B* indicate increasing time/color sequence. The arrows indicate the relative orbital angular rates. The "/" and "\" indicate the resulting arm winding senses. The $36.5''$ CR sequences are also indicated.

reveals two weaker CCW inner arms winding opposite the outer pair. One of this inner pair is outlined with black dots. *NGC4622 thus must have a pair of leading arms, either the weak inner or strong outer pair. Note that we do not use the Figure 2 rotation curve to reach this conclusion, nor is it even necessary to assume that the galaxy is at equilibrium. More specifically, we do not have to assume that the galaxy is not changing much over time spans like the orbital period at CR.*

Fourier decomposition in different color bands can also be used to identify CR radii without using the Figure 2 rotation curve. Before we examine the Fourier images in different color bands, we will examine Figure 1 and its inset in more detail. We noted earlier that blue stellar associations to the left of the "1" are displaced on the concave side of the arm. Proceeding farther to the left inward of the number 1, the string of associations is progressively closer to the middle of the stellar arm with the bright association toward the left edge of the large frame, being close to the middle of the stellar arm. In the inset going from the left outward toward the number 2, the associations are on the convex side of the arm but tend toward the middle as the number 2 is approached. This is just what one would expect if there were a CR radius at about $36''$ between arms 1 and 2. Near CR, the orbital and pattern angular rates are nearly the same and in the same sense, so there will be no *IVB* color/age displacement, but the formation of a large association toward the middle of the stellar arm might be promoted.

Use of the Fourier components in *IVB* permits a determination of CR radii over more of the disk with greater confidence. Let us look at the arms as revealed in a graph of the position angle (positive CCW on the sky) of the maximum intensity peak of the $m = 2$ Fourier component versus radius of the images. One can determine the position angle of the peak amplitude for each of the *IVB* bands as one steps around the disk. Figure 6 shows the position angle versus radius of the $m = 2$ *IVB* intensity maxima for two radius ranges in the galaxy. Figure 6 top shows a strong $m = 2$ *IVB* order switch at radius $= 21.4''$. Inside this radius, the *IVB* sequence is CW; outside that radius the *IVB* sequence is CCW. We thus presume that there is a CR radius at $21.4''$. Figure 6 bottom shows a weaker $m = 2$ *IVB* order switch at radius $= 36''$. Inside this radius, the *IVB* sequence is CCW; outside that radius the *IVB* sequence is CW. We thus presume that there is a CR radius at $36''$.

Up to now we have established that NGC4622 must have a leading pair of arms along with two CR radii without using the rotation curve. However, we do not yet know which arms lead, the inner pair and single or the outer pair and single. To find which arms lead in NGC4622, we will now use the best-established feature of the rotation curve, the decline of the orbital angular rate with radius crossing $21.4''$. Figure 7 shows a diagram of the two presumed CR radii, the relative *IVB* sequences at each, and the relative orbital angular rates. Referring to Figure 7, we interpret the *IVB* switching crossing

21.4″ as the CR radius of a two-fold component of a rotating perturbation in the disk. Since the observed angular velocity declines across the 21.4″ radius, the disk orbit sense on the sky must be CW. As noted earlier, to the left of point 2 in the Figure 1 inset just outside 21.4″ there is a CCW displacement of blue newly formed stars relative to the smooth stellar arm. This displacement confirms the location of the CR radius and a CW disk orbit sense on the sky. *If the orbit angular rate declines with radius in this region and the pair of arms starting at about 25″ winds outward in a CW sense, they must be a leading pair.*

The orbital angular rate (circular velocity/radius) determines the pattern speed which produces CR at the radius of the color sequence reversal at 21.4″. In the neighborhood of 21.4″ the rotation curve has a declining orbital angular rate. Using the rotation curve given earlier, a pattern speed of about 6.5 (km s^{-1})/″ has a CR radius at the $r = 21.4''$ boundary between the inner arm and the ring. We interpret this as the pattern speed for the $m = 2$ and (as we shall see later) the $m = 1$ disturbances. We have indicated this pattern speed in the Figure 3 orbital angular velocity plot with a horizontal line at about 6.5 (km s^{-1})/″. The co-rotational coincidence of the pattern speed with the orbital angular rate at 21.4″ is marked with a vertical dashed line in the figure.

Note in the bottom half of Figure 6 that the $m = 2$ *IVB* peaks also weakly switch their order at radius = 36.5″ with *IVB* CCW inside and CW outside that radius. This may be due to the rising rotation curve's angular rate rising at this radius to again equal the pattern speed. Look in Figure 3 and see how, after crossing the CR radius at 21.4″, at about 25″ the angular rate curve possibly starts to climb with radius (dashed line) so that it will again cross the pattern speed horizontal line at a larger radius. The Figure 3 crossing radius would be larger than 36.5″, but the rotation curve and orbital angular rate values in this region are not precisely known. Figure 5 gives the *HST* $m = 2$ Fourier component image with one of the outer pair of CW (presumably leading) arms marked with a line of white dots. Inside about 25″ the orbital angular rate probably declines with increasing radius. We see that there are a pair of CCW (presumably trailing) inner arms. One of these is marked with a row of black dots. The arm sense switch between the two angular rate regions is what we would expect. In a normal photograph such as Figure 1, we do not see the weak CCW inner pair of arms because the single arm dominates in that inner region.

6. NGC4622 FOURIER IMAGES AND LEADING/TRAILING $m = 1$ ARMS

Fourier decomposition can provide an independent method to that of paper I to ascertain that a single arm in NGC4622 definitely leads. Figure 8 shows an *I*-band image of the Fourier $m = 1$ component of NGC4622. This filtering process reveals the underlying stellar disk, showing the inner single CCW arm. In addition to the single bright inner arm, note that the $m = 1$ image reveals a weaker CW inner arm winding opposite the inner bright arm. This faint outer arm is outlined with black dots. Note that this outer single CW (winding outward) arm is hidden in the normal Figure 1 image by the dominant pair of outer CW arms. *NGC4622 thus must have a single leading arm, either the strong inner or weak outer. Note that we do not use the Figure 2 rotation curve to reach this conclusion.*

Fourier decomposition in different color bands of the $m = 1$ image can also be used to identify CR radii without using the Figure 2 rotation curve. Figure 9 gives the *HST* $m = 1$ Fourier component position angle versus radius for the inner 40″ of the disk. We see additional support for 21.4″ being the CR radius in the 180° phase jump at that radius. As can be deduced from Equation (9) of Byrd et al. (2006), at CR this phase jump occurs for an $m = 1$ perturbation.

The *HST* $m = 1$ Fourier component position angle versus radius is most straightforwardly interpreted in terms of perturbed orbital motion inside and outside the CR radius. In the case of the single arm, the $I - B$ peaks spread out in position angle because the angular motion of the inner single arm perturbation pattern

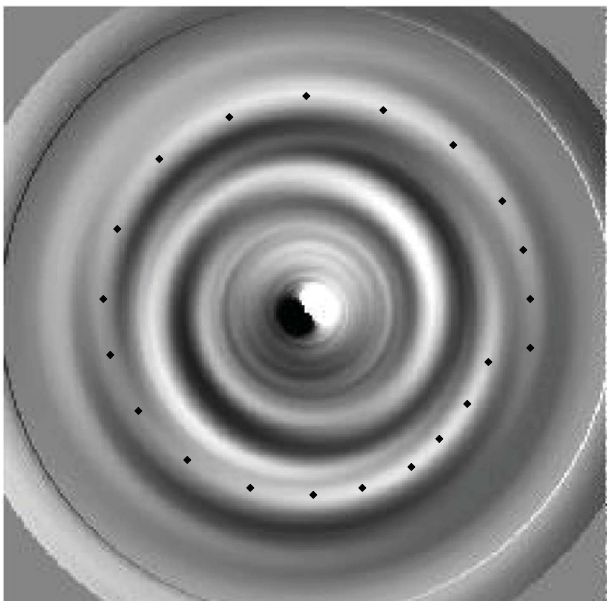

Figure 8. The $m = 1$ Fourier image of NGC4622. The inner single arm winds outward in a CCW direction. Beyond the CR radius of 21.4″, a weaker single arm pattern (marked with dots) winds out in an opposing CW direction like the outer pair of arms.

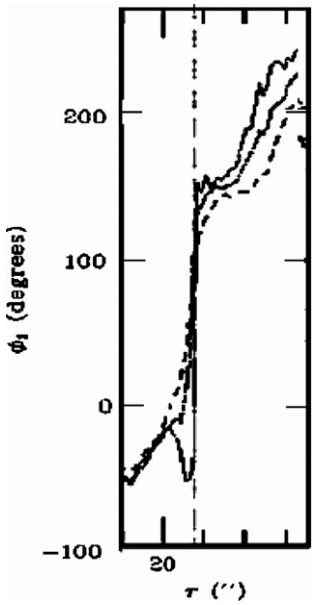

Figure 9. The $m = 1$ Fourier component position angle versus radius. The phases of the *IVB* peaks versus radius are shown. The vertical dashed line marks the CR radius of the pattern speed. The 180° phase jump is a characteristic of the $m = 1$ CR resonance.

speed is slower than the orbital motion of the disk. Referring back to the Figure 6 diagram and Figure 9, the position angles of the peaks form an *IVB* "light up" sequence as one steps around the disk in *decreasing* (CW) position angle inside 21.4″. Outside 21.4″, the position angles of the peaks form a *IVB* sequence as one steps around the disk in *increasing* (CCW) position angle. We thus see evidence from the single arms that 21.4″ is a CR radius.

Up to now, we have established with the $m = 1$ images that NGC4622 must have a leading single arm along with at least one CR radius. However, we do not yet know which leads, the inner or the outer single arm. To find which leads in NGC4622, we will again use the best established feature of the rotation curve, the decline of the orbital angular rate with radius crossing 21.4″. Referring to Figure 7 again, we interpret the *IVB* switching crossing 21.4″ as the CR radius of a one-fold component of a rotating perturbation in the disk. Since the observed angular velocity declines across the 21.4″ radius, the disk orbit sense on the sky must be CW. *If the orbit angular rate declines with radius in this region and the inner single arm winds outward in a CCW sense, it must be a trailing arm. Conversely, the single outer arm winding outward in a CW sense (marked with black dots in Figure 8) must be a leading arm.*

The orbital angular rate determines the pattern speed which produces CR at the radius of the $m = 1$ phase jump and color sequence reversal at 21.4″. In the neighborhood of 21.4″ the rotation curve has a declining orbital angular rate. Using the rotation curve given earlier, a pattern speed of about 6.5 (km s^{-1})/″ has CR at $r = 21.4''$. We interpret this as the pattern speed for the $m = 1$ and $m = 2$ perturbations as indicated with a horizontal line at about 6.5 (km s^{-1})/″ and a vertical line at 21.4″. Assuming the Figure 3 observational curve, we thus have evidence for a strong outer leading pair of arms and a strong inner trailing single arm.

7. CO-ROTATION RADII FROM ARM POTENTIAL-DENSITY PHASE SHIFTS

Zhang & Buta (2007) have outlined a new method for locating the CR radii of density waves (bars and spirals) in disk galaxies. The method is based on the radial distribution of an azimuthal phase shift between the density inferred from a near-infrared image and the potential implied by that density. Zhang & Buta show that the expected phase shift between the density inferred from our *I*-band *HST* image and the potential in NGC4622 provides further corroboration of the leading sense of the main outer arms. Positive to negative phase shift crossings, interpreted as CR radii, occur at 24″ and 36″ if the disk rotates clockwise. These are similar to both our paper I findings and our results here. The potential-density phase shift results are consistent with the *IVB* trends we have found here and in paper I if the outer arms lead.

8. CONCLUSIONS

Using *HST* and ground-based observations, paper I's dust silhouette method determines that the disk of NGC4622 rotates CW on the sky. The outer pair of arms winding outward CW on the sky should thus lead (wind outward in the direction of disk orbital motion), contrary to most expectations. NGC4622's moderate (19°) tilt is a plus for the independent methods we use in the present paper to verify our earlier conclusions. We find that $m = 2$ Fourier component images show an additional inner weaker CCW pair of arms as well as the already-known strong outer CW pair. NGC4622 must have a pair of leading arms in the inner or the outer regions, with no need to know the rotation curve. In addition to the strong, already-known, CCW single inner arm, we see a weaker outer single CW arm component. We conclude that NGC4622 must have a single leading arm component in the inner or the outer parts, with no need to know the rotation curve.

We use the *IVB* color/age method to locate CR radii. At CR, the Fourier position angle peaks switch position angle sequence (e.g., *IVB* to *BVI* or the reverse). To use the *IVB* method, we assume that NGC4622 disk and the arm pattern speed does not change greatly over times comparable to the circular orbital period (∼190 million years) at CR.

We find two possible CR radii at 21.4″ and 36″. The boundary between the outer CW arms and the inner CCW arms is between these two radii. From the *IVB* switching and the observed orbital angular rate decline crossing the first CR radius, the orbit sense is CW and the outer pair is the leading pair. Using the observed rotation curve and the CR radius, the pattern speed must be about 6.5 (km s^{-1})/″. For the $m = 2$ and $m = 1$ the CR radius is at 21.4″. By methods independent of those in paper I, we place on a firm footing our earlier conclusions about the unusual nature of the NGC4622 spiral pattern. Additional study of this very unusual galaxy should help illuminate the mechanisms of spiral arm formation and properties of disk galaxies.

This work was supported by NSAS/STScI grant 8707 to the University of Alabama and NSF grant AST 02-0177 to Bevill State College in Fayette, Alabama. R.B. acknowledges the support of NSF grant AST 050-7140.

REFERENCES

Athanassoula, E. 1978, A&A, 69, 395
Binney, J., & Tremaine, S. 1987, Galactic Dynamics (Princeton, NJ: Princeton Univ. Press)
Buta, R., Crocker, D., & Byrd, G. G. 1992, AJ, 103, 1526
Buta, R., Byrd, G. G., & Freeman, T. 2003, AJ, 125, 634
Byrd, G. G., et al. 1989, Celest. Mech., 45, 31
Byrd, G. G., Freeman, T., & Buta, R. 2006, AJ, 131, 1377
Byrd, G. G., Freeman, T., & Howard, S. 1993, AJ, 105, 477
de Vaucouleurs, G. 1958, ApJ, 127, 487
Hubble, E. 1943, ApJ, 97, 112
Keel, W. C. 1991, ApJ, 375, L5
Lindblad, B. 1941, Stockholms Observatoriums Annaler, bd. 13, no 10 (Stockholm: Almqvist & Wiksell), 3
Puerari, I., & Dottori, H. 1997, ApJ, 476, L73
Thomasson, M., Donner, K. J., Sundelius, B., Byrd, G. G., Huang, T. Y., & Valtonen, M. J. 1989, A&A, 211, 25
Vera-Villamizar, N., Dottori, H., Puerari, I., & de Carvalho, R. 2001, ApJ, 547, 187
Zhang, X., & Buta, R. J. 2007, AJ, 133, 2584